NEUROSCIENCE

The hippocampal engram maps experience but not place

Kazumasa Z. Tanaka[1]*, Hongshen He[1,2], Anupratap Tomar[1]†, Kazue Niisato[1], Arthur J. Y. Huang[1], Thomas J. McHugh[1,2]*

Episodic memories are encoded by a sparse population of hippocampal neurons. In mice, optogenetic manipulation of this memory engram established that these neurons are indispensable and inducing for memory recall. However, little is known about their in vivo activity or precise role in memory. We found that during memory encoding, only a fraction of CA1 place cells function as engram neurons, distinguished by firing repetitive bursts paced at the theta frequency. During memory recall, these neurons remained highly context specific, yet demonstrated preferential remapping of their place fields. These data demonstrate a dissociation of precise spatial coding and contextual indexing by distinct hippocampal ensembles and suggest that the hippocampal engram serves as an index of memory content.

Numerous theories have attempted to link the physiology of the hippocampus with its role in episodic memory (*1*, *2*); however, experimental tests of these ideas remain scarce. One prevailing model suggests that the hippocampal memory trace contains rich information about the animal's current location within the cognitive domain, providing a spatial framework on which events and items can be anchored and related [cognitive map theory (*3*, *4*)]. This model is supported by data demonstrating that synaptic plasticity stabilizes these hippocampal maps and that animals can reliably recall these representations, even at remote time points (*5*, *6*). An alternative, although not mutually exclusive, hypothesis, the memory index theory, asserts that the hippocampal memory trace is primarily an index that provides rapid and efficient access to the content of an episodic memory stored in the neocortex (*7*, *8*). This theory is agnostic to the information content in the hippocampus, emphasizing its role in reactivating downstream cortical modules, with plasticity serving to establish a link between the hippocampal index and the neocortical activity pattern.

Although place cell physiology supports the cognitive map theory (*9*), behavioral studies using contextual fear conditioning [CFC (*10*)] may be better interpreted via the memory index theory. In CFC, the contextual representation is index-like because its formation requires conjunctive exposure to cues and its rapid recall does not require physical exploration of the environment (*11*). Moreover, the expression of activity-induced genes, such as c-*Fos*, is rapidly and robustly induced in a specific neuronal ensemble after presentation of novel configurations of stimuli and is thought to define the neuronal substrates of the contextual representation (*12*, *13*). Recent studies (*14*) further strengthen this view, demonstrating that inhibition of hippocampal engrams can block memory recall in contextual tasks, whereas activation can drive context-triggered behavior (*15*, *16*). The link between this contextual memory representation and precise locations or routes represented by place cells during exploration remains unknown.

We therefore conducted tetrode recordings from CA1 pyramidal cells in freely moving c-FostTA (tetracycline-transactivator) transgenic mice infused with virus expressing channelrhodopsin2 and enhanced yellow fluorescent protein under the control of the Tet-responsive element (AAV-TRE-ChR2-EFYP). Doxycycline was removed from the diet of the mice, triggering labeling of c-Fos–expressing (positive) cells with ChR2, and place cell activity was recorded as mice explored a novel context (A; encoding context; Fig. 1A). The next day (12 to 14 hours later; fig. S1), the animals were reexposed to context A (recall) to examine the stability of the spatial map. CA1 was stimulated with pulses of blue light (10 mW, 0.5 Hz, 15 ms) to identify the subset of cells that expressed ChR2 as a result of c-Fos expression during the first session (Fig. 1B and fig. S2). In a separate cohort of mice, we verified that this OptID protocol did not affect excitability or spatial coding properties of the labeled neurons (fig. S3). Across the seven animals used in this study, 19.59 ± 2.65% of putative pyramidal cells exhibited light-induced spikes and thus were identified as c-Fos positive (Fig. 1C). This fraction is consistent with previous reports (*17*). Finally, the same mice explored a distinct environment (B) to examine context-specific activity (*18*).

We first examined the spatial firing of c-Fos–positive neurons as the animals explored the novel context A. The majority (79.31%) of these cells had place fields in the labeled context (Fig. 1D; see methods for place field criteria). However, a large fraction (75.53%) of the active place cells were not labeled with ChR2 (Fig. 1E). Although physiologically similar, with indistinguishable peak firing rates (Fig. 1F; pos: 6.99 ± 1.06 Hz; neg: 6.06 ± 0.53 Hz, $W = 640$, $p = 0.20$), c-Fos–positive place cells exhibited significantly higher mean firing rates (Fig. 1G; pos: 1.43 ± 0.22 Hz; neg: 0.77 ± 0.11 Hz, $W = 357$, $p = 5.4 \times 10^{-5}$). Accordingly, positive cells had larger place fields (Fig. 1H; pos: 28.00 ± 3.50 cm^2; neg: 17.97 ± 1.79 cm^2, $W = 517$, $p = 0.0085$) and on average, their spikes carried lower spatial information (Fig. 1I; pos: 0.69 ± 0.81 bits/spike; neg: 1.21 ± 0.83 bits/spike, $W = 1191$, $p = 0.001$).

We next analyzed the temporal structures of spike activity during exploration (A, encoding). Interspike interval (ISI) analysis revealed that spikes from engram cells were more likely to occur in bursts (3- to 15-ms ISI) (Fig. 2A). These neurons had significantly higher burst rates (Fig. 2B; pos: 16.80 ± 3.04 bursts/min; neg: 8.87 ± 1.44 bursts/min, $W = 1243$, $p = 0.00018$) and shorter average interburst intervals (IBIs) (Fig. 2C; IBI: pos: 6.55 ± 1.30 s; neg: 16.27 ± 2.15 s, $W = 415$, $p = 0.00042$). Burst events in c-Fos–positive neurons were preferentially spaced at ~125 ms, an interval corresponding to the 8-Hz theta rhythm in the hippocampus; thus, bursts from these neurons were significantly more theta modulated than bursts from c-Fos–negative cells (Fig. 2, D to F; theta modulation index, $W = 418$, $p = 0.0009$; theta power in burst spectrum, $W = 1151$, $p = 4.8 \times 10^{-5}$). We defined theta-burst events (TBEs) as bursts repeated at IBIs of 83 to 167 ms (6 to 12 Hz) and compared this property across the groups. During exploration of the novel context A, c-Fos–positive cells showed higher rates of TBEs than c-Fos–negative place cells (Fig. 2, G and H; pos: 5.44 ± 1.41 bursts/min; neg: 2.58 ± 0.53 bursts/min; $W = 417.5$, $p = 0.00046$) and longer repetitions of bursts (Fig. 2, I and J; pos: 2.68 ± 0.095 bursts/event; neg: 2.56 ± 0.052 bursts/event; $W = 652.5$, $p = 0.20$; Fig. 2I, max TBE length: pos: 7.13 ± 0.78 bursts; neg: 5.28 ± 0.34 bursts, $W = 542$, $p = 0.022$). These burst features were no longer prominent in ChR2-labeled neurons when the animals explored context B (fig. S5), suggesting their involvement in contextual encoding.

We then examined the temporal modulation of place cell spiking by the oscillatory population activity in the local field potential (LFP) (A, encoding). CA1 neurons can be entrained by the theta (6 to 12 Hz) rhythm, as well as by slow (30 to 50 Hz) and fast (55 to 85 Hz) gamma oscillations, which correlate with CA3 and entorhinal cortical inputs to CA1, respectively (*19*). Spikes from c-Fos–positive and –negative cells were similarly theta entrained and preferred the ascending phase of the oscillation (Fig. 3, A and B; mean preferred phase, pos: 229.9 ± 1.73°; neg: 199.2 ± 1.85°, $W = 0.42$, $p = 0.81$). However, TBE spikes in positive neurons preferentially occurred during the descending phase, whereas those in negative neurons remained locked to the ascending phase (Fig. 3, C to E; mean

[1]Laboratory for Circuit and Behavioral Physiology, RIKEN Center for Brain Science, 2-1 Hirosawa, Wakoshi, Saitama, Japan. [2]Department of Life Sciences, Graduate School of Arts and Sciences, University of Tokyo, Tokyo, Japan.
*Corresponding author. Email: kazumasa.tanaka@riken.jp (K.Z.T.); thomas.mchugh@riken.jp (T.J.M.)
†Present address: School of Physiology, Pharmacology and Neuroscience, University of Bristol, Bristol, UK.

preferred phase: pos: 170.7 ± 1.86°; neg: 325.7 ± 1.54°, $W = 62.66$, $p = 2.5 \times 10^{-14}$). Next, to address any differences in coupling of positive and negative neurons to CA1 inputs, we examined spikes during gamma events. Significantly more spikes from positive neurons occurred during fast gamma events, and a larger fraction of these neurons were phase locked to fast gamma oscillations compared to the c-Fos–negative population (Fig. 3F; percentage of spikes: pos: 2.62 ± 0.17%; neg: 2.19 ± 0.11%, $W = 1067$, $p = 0.0072$; percentage of phase-locked cells: pos: 26.09%; neg: 14.08%, chi-squared test, $p = 0.0014$). There was no significant difference in spiking or phase locking between the groups during slow gamma (Fig. 3G; percentage of spikes: pos: 5.81 ± 0.31%; neg: 5.53 ± 0.23%; $W = 888$, $p = 0.53$; percentage of phase-locked cells: pos: 26.09%; neg: 29.58%, chi-squared test, $p = 0.62$). These data suggest that although both populations of neurons are similarly tuned to CA3-driven excitation, c-Fos–positive neurons may be more responsive to input from the entorhinal cortex, resulting in the temporal shift in their distinctive theta-paced bursting.

Finally, we examined hippocampal activity during memory recall and assessed the stability of the spatial representation of engram cells when animals revisited the labeling context (A). Contrary to expectations of a spatial memory trace, many of these cells shifted their firing locations during the second visit (Fig. 4A and fig. S6). In positive neurons, the average correlation of the firing-rate maps from the encoding and recall sessions was close to zero, significantly lower than that from negative place cells (Fig. 4B; pos: 0.079 ± 0.070; neg: 0.31 ± 0.052, $W = 560$, $p = 0.010$). However, correlations of the mean firing rate, independent of position, were similar across both populations of cells (Fig. 4C; pos: 0.36 ± 0.053; neg: 0.36 ± 0.029, $W = 412$, $p = 0.81$), suggesting that c-Fos–positive neurons represent contextual information in a different manner. Therefore, we examined their activity in a distinct context. When animals explored context B, many c-Fos–positive cells remained silent (Fig. 4A and fig. S6; 43.5% of positive place cells had a peak rate of <1 Hz in context B; peak

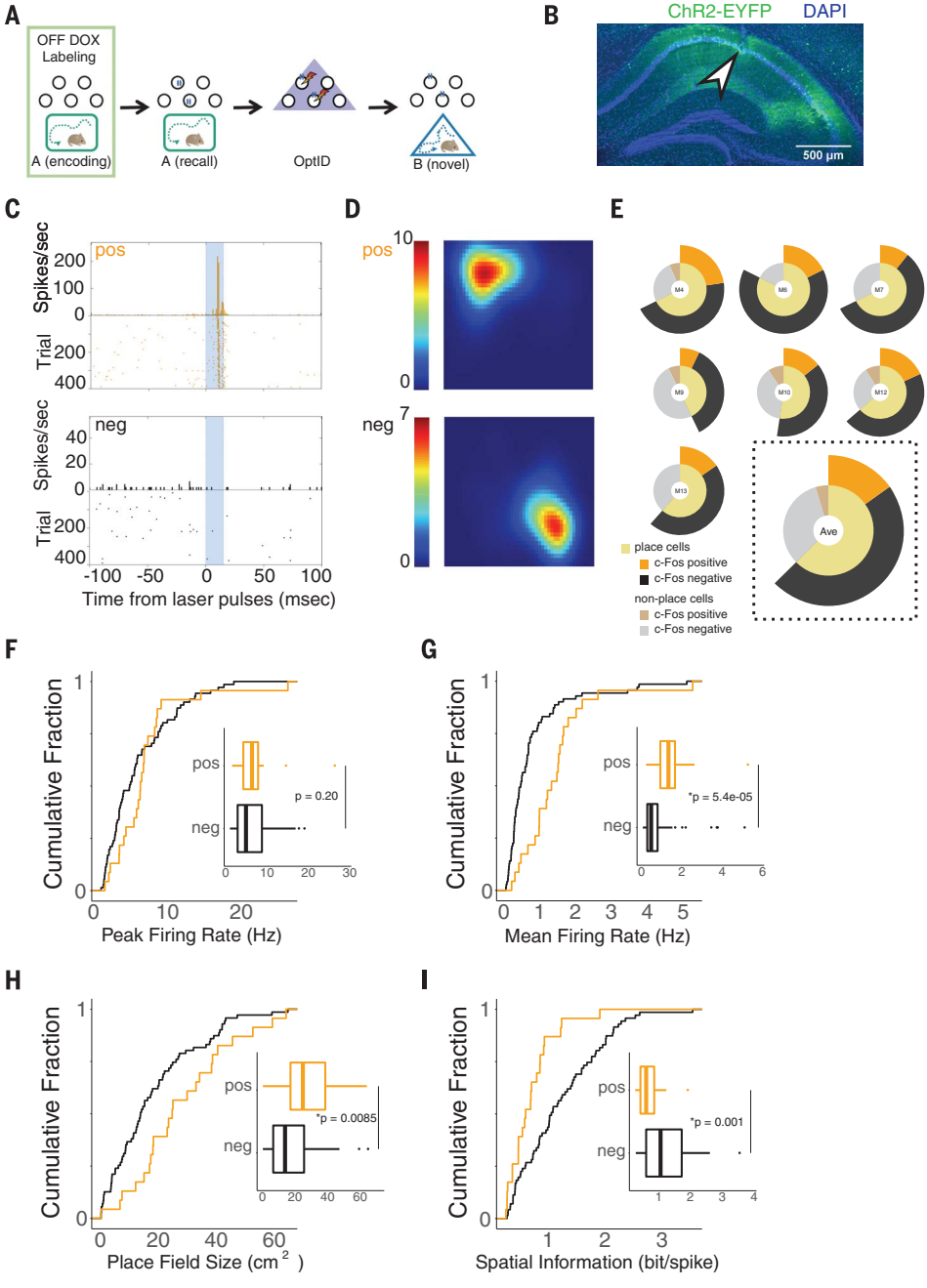

Fig. 1. c-Fos induction in a fraction of place cells during exploration of a novel context. (**A**) A schematic of the experimental protocol. Mice were exposed to a novel context (A, encoding) when doxycycline was removed from the diet (OFF DOX), followed by reexposure to the same context (A, recall). Twenty-four hours after A (encoding), labeled cells were identified through light-induced spikes. Finally, mice explored a distinct context B (novel). (**B**) A representative image of ChR2-EYFP (green) expression in the dorsal CA1 of the hippocampus. The white arrowhead indicates a tetrode location. DAPI, 4′,6-diamidino-2-phenylindole. (**C**) Peristimulus time histogram of representative single units classified as c-Fos–labeled (pos) or not labeled (neg). Blue area represent light on epoch (15 ms). (**D**) Firing-rate maps of representative place cells showing location-specific firing during exploration in context A (encoding). (**E**) Pie plots describing percentages of each cell type in recorded animals ($N = 7$), and their average (dashed square). (**F** to **I**) Cumulative density plots with inset box plots comparing peak firing rates (F), mean firing rates (G), place field size (H), or spatial information (I) between c-Fos–positive (orange) and –negative (black) place cells. Box plots show median, first, and third quantiles, and minimum and maximum values within 1.5× the interquantile range (IQR) from each quantile.

firing rate in context A: 6.99 ± 1.06 Hz; context B: 3.42 ± 0.76 Hz, W = 392, p = 0.005). Consequently, there were fewer c-Fos–positive place cells, and the spatial information of these neurons was smaller than in context A (Fig. 4D, Friedman rank sum test, Friedman chi-squared = 6, p = 0.014; two-way analysis of variance, significant interaction, $F_{(1,89)}$ = 4.9, p = 0.029; Fig. 4E, spatial information: context A: 0.89 ± 0.21 bit/s; context B: 0.32 ± 0.071 bit/s, W = 396, p = 0.0033). By contrast, the average spatial information carried by c-Fos–negative place cells was unchanged (Fig. 4F; context A: 0.51 ± 0.064 bit/s; context B: 0.37 ± 0.044 bit/s, W = 2643, p = 0.30), although these cells typically shifted the location of their spatial firing ("remapped") in the new context (Fig. 4G; spatial correlation, A/A: 0.31 ± 0.052; A/B: 0.013 ± 0.052, W = 982, p = 0.00029). These data are consistent with the hypothesis that engram cells do not necessarily represent reliable spatial information about the external world, but rather through their net activity serve as an index to episodic information stored elsewhere in the brain (*7*, *8*). We therefore sought to discriminate

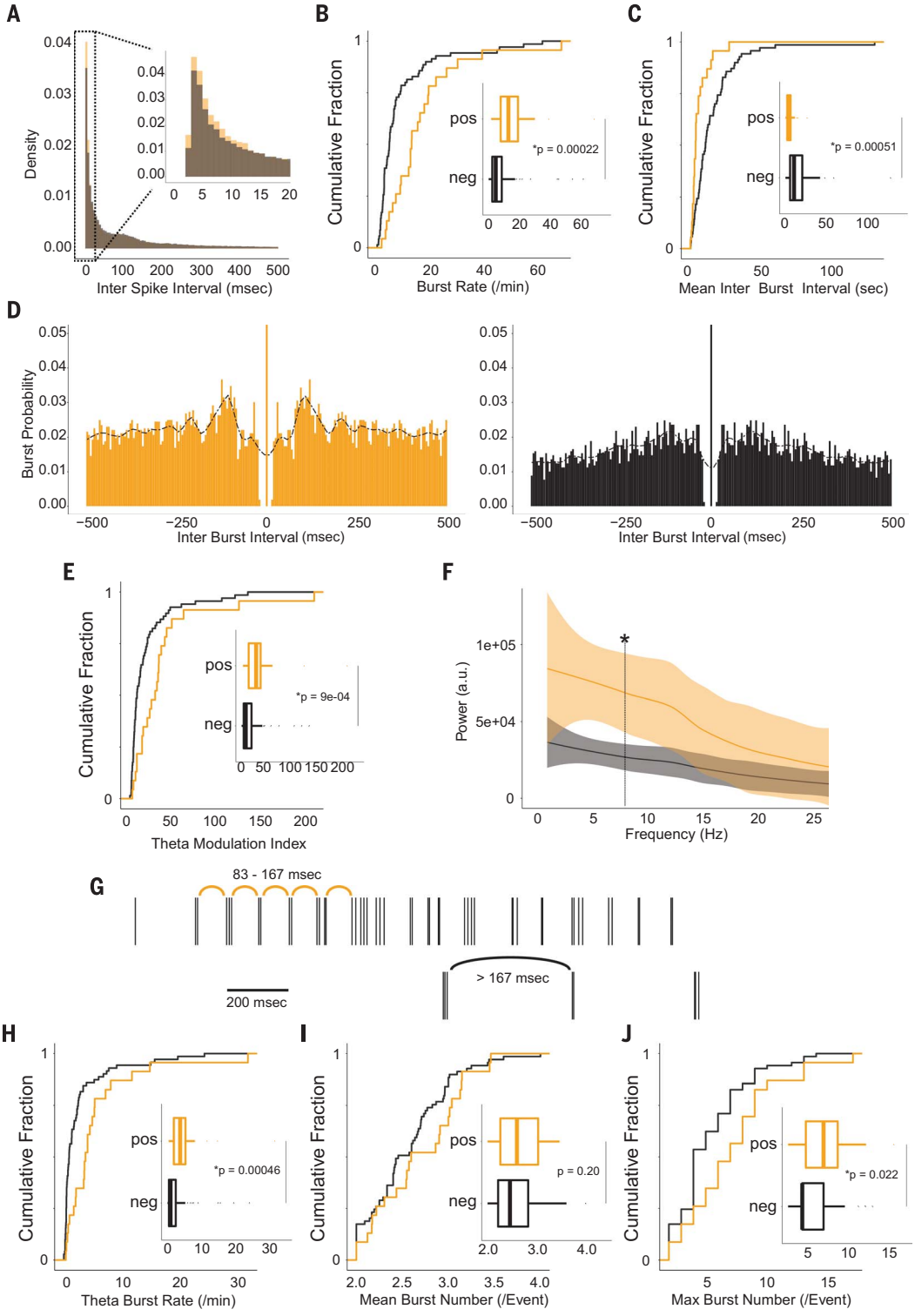

Fig. 2. Theta-paced burst activity in c-Fos–positive place cells. (**A**) Histograms showing densities of interspike intervals from all c-Fos–positive (orange) or –negative (black) place cells. (**B** and **C**) Cumulative density plots and box plots comparing burst rates (B) and mean interburst intervals (C) of the two cell types. (**D**) Autocorrelogram of burst activity from an example positive (orange) and negative (black) place cell. Local polynomial regression lines are plotted over the histograms. (**E**) Theta modulation index of burst autocorrelograms. (**F**) Power spectrograms of burst trains. Vertical line denotes 8 Hz. (**G**) Example raster plots showing theta-paced burst events (TBEs; IBI = 83 to 167 ms) and repetitive bursts outside of the criteria (IBI < 83 ms or IBI > 167 ms). (**H** to **J**) Cumulative density plots and box plots comparing TBE rates (H), mean burst number per TBE (I), and maximum burst number within a single TBE (J) of the two cell types. Box plots show median, first, and third quantiles, and minimum and maximum values within 1.5× the IQR from each quantile.

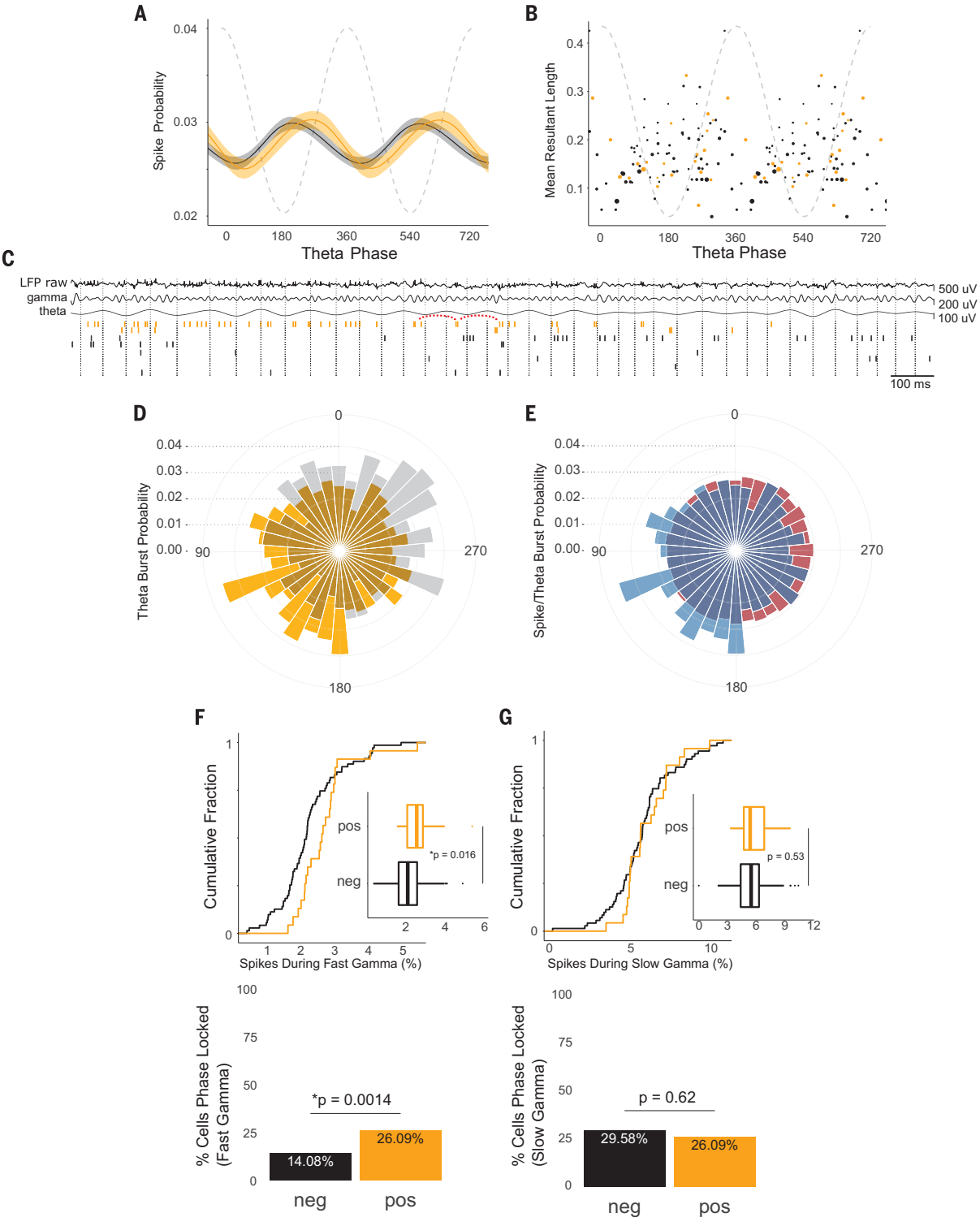

Fig. 3. LFP modulation of spikes from c-Fos–positive and –negative place cells. (**A**) Spike probability of the two types of cells over phases of theta oscillation (6 to 12 Hz) [positive (orange) or negative (black); only significantly phase-locked cells were used]. Envelopes represent confidence intervals; the dashed line represents theta. (**B**) Mean resultant length of c-Fos–positive (orange) or –negative (black) cells plotted as a function of preferred theta phase. Dot size represents mean firing rate of that cell. Only significantly phase-locked cells are plotted (positive: 22 cells; negative: 68 cells). (**C**) Example spike raster plots with LFP traces [raw, theta filtered (6 to 12 Hz), gamma filtered (30 to 85 Hz)]. Red arcs represent a TBE occurring at the descending phase of theta. (**D**) A rose plot showing TBE spike probability across theta phases [positive (orange) or negative (black), 10° bins]. (**E**) A rose plot showing spike probability of c-Fos–positive place cells over theta phases (TBE spikes are in blue, all spikes in red). (**F**) Percentage of spikes occurring during fast gamma events (top), and percentage of cells phase locked to fast gamma oscillations [bottom; positive (orange) or negative (black)]. (**G**) Percentage of spikes occurring during slow gamma events (top), and percentage of cells phase locked to slow gamma oscillations [bottom; positive (orange) or negative (black)].

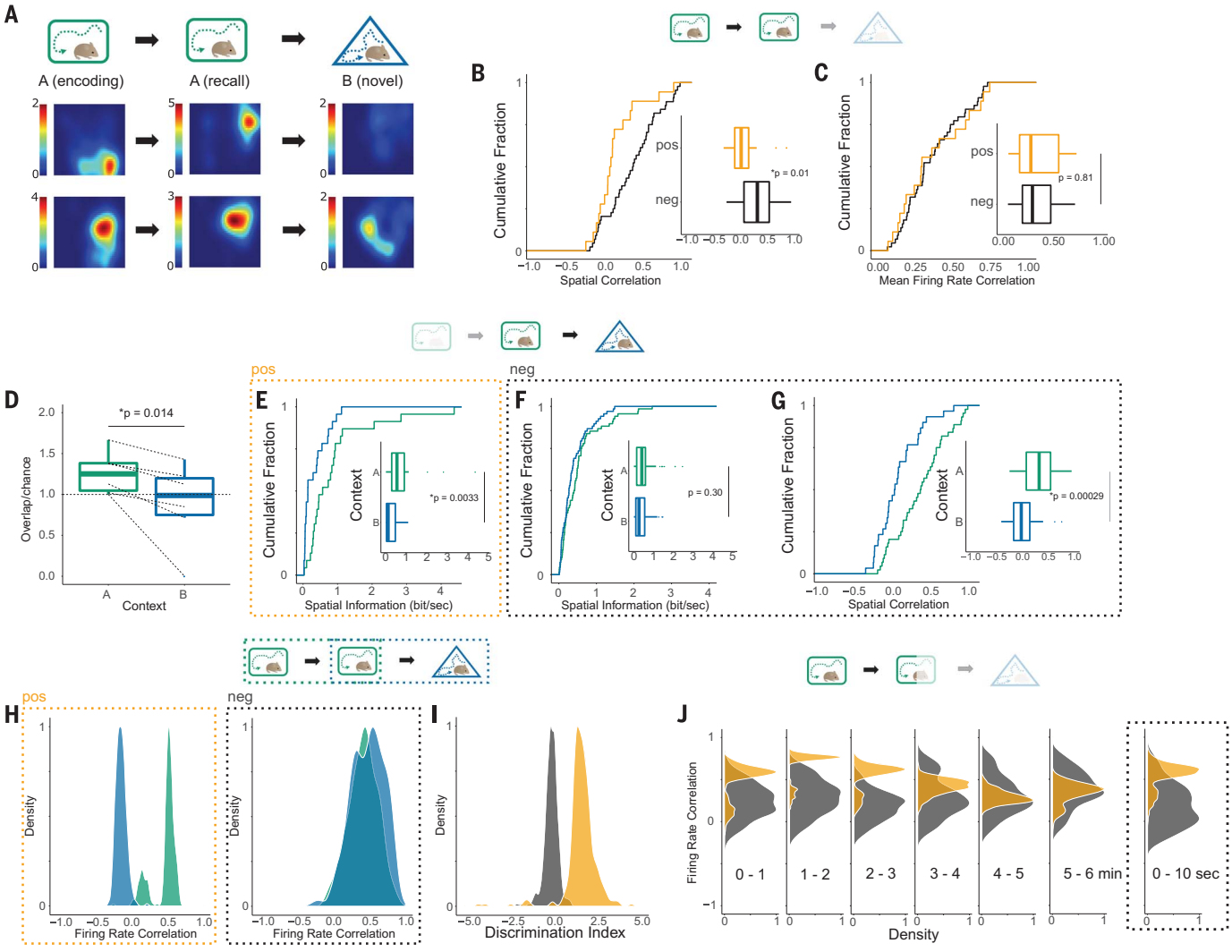

Fig. 4. Different responses of c-Fos–positive and –negative place cells to the encoding context and a distinct novel context. (**A**) Firing-rate maps of c-Fos–positive (top) or –negative (bottom) place cell activity during encoding (left), reexposure to the encoding context (middle), or exploration of a distinct novel context (right). (**B**) Spatial correlation between place maps in A (encoding) and A (recall) [positive (orange) or negative (black)]. (**C**) Mean firing-rate correlation between place maps in A (encoding) and A (recall) [positive (orange) or negative (black)]. (**D**) An animal-by-animal box plot showing observed overlap between c-Fos–positive cells and place cells normalized by those expected by chance, comparing context A (encoding, green) versus B (novel, blue) sessions. Spatial information of (**E**) c-Fos–positive or (**F**) c-Fos–negative place cells when animals explore context A (encoding; green) or B (novel; blue). (**G**) Spatial correlations of c-Fos–negative place cells in A (encoding; green) and B (novel; blue). (**H**) Distribution of ensemble firing-rate correlations of c-Fos–positive or –negative place cells between context A (encoding) – A (recall) (green) versus A (encoding) – B (novel) (blue). (**I**) Distribution of discrimination indexes obtained by c-Fos–positive (orange) or –negative (black) ensemble firing-rate correlations. (**J**) Instantaneous ensemble firing-rate correlations of the initial 6 min of the context A (recall) session binned by 1 min (left), or that of the first 10 s (right). c-Fos–positive place cells are in orange, c-Fos–negative cells in black. For (H) to (J), values are plotted as probability densities (scaled). Box plots show median, first, and third quantiles, and minimum and maximum values within 1.5× the IQR from each quantile.

contexts only from firing-rate correlations of a subpopulation of neurons. We randomly subsampled c-Fos–positive neurons and an equivalent number of c-Fos–negative place cells and calculated the correlation of the mean firing rates of each population between context A (encoding) and A (recall) or between context A (encoding) and B (novel), repeating the procedure 1000 times (see methods). As a population, the firing rate of c-Fos–positive place cells reliably discriminated the two contexts, whereas the firing rate of the ensemble of negative cells did not (Fig. 4H; probability of finding a higher correlation in A/B than A/A, $p = 0.002$ for positive ensemble, $p = 0.57$ for negative ensemble). This was also evident in the discrimination index (Fig. 4I; probability of finding a greater index in the negative than the positive ensemble, $p = 0.049$). In contrast to the negative ensemble, context discrimination from firing-rate correlations of c-Fos–positive cells was prominent early in the recall session, demonstrating high correlation to the average rate of the encoding session during the first few minutes, or even the first 10 s (Fig. 4J and fig. S7; probability of finding a higher correlation in the negative than the positive ensemble, $p = 0.055$, 0.038, 0.011, 0.230, 0.906, and 0.754 for 1- to 6-min bins, $p = 0.046$ for the first 10-s bin), suggesting the rapid reactivation of contextual representation by the subset of engram neurons. These data demonstrate that engram cells are place cells with lower spatial stability and accuracy, but with activity that can reliably and quickly reflect contextual identity.

When animals explore a novel context, an engram is formed by a fraction of the place cells,

suggesting that the plasticity involved in engram formation is distinct from that for formation of place fields. During encoding in the labeled context, engram neurons demonstrate repetitive theta-frequency bursts. In vitro, this pattern of action potentials is known to produce a form of long-term potentiation mediated by brain-derived neurotrophic factor (BDNF) secretion and dependent on c-Fos expression (*20*, *21*). c-Fos expression and theta bursts have been observed in CA1 when animals perform a non–spatial memory task (*22*, *23*), suggesting that this activity may be a signature of hippocampal engrams indexing broader types of memories.

Our study does not support the idea that the hippocampal engram simply encodes spatial memory because these neurons do not maintain their firing locations in the same environment across time. Instead, we propose that these cells may serve as an index for contextual memory through a shift of firing rates. Compared to other place cells, during recall these c-Fos–positive neurons rapidly spike at rates that are highly correlated to their activity during the encoding period and are preferentially silent in a distinct context. This feature may explain why optogenetic stimulation of the hippocampal engram can influence contextual memory recall (fig. S8) (*24*), despite lacking temporally meaningful pattern of spikes. Inhibition of the CA1 engram reduces downstream cortical reactivation (*25*), consistent with a role in indexing. Our data suggest that specific ensembles of hippocampal neurons simultaneously support distinct domains of episodic memories—spatially reliable c-Fos–negative neurons for configurational coding and spatially unstable engrams for contextual indexing.

REFERENCES AND NOTES

1. M. L. Shapiro, H. Eichenbaum, *Hippocampus* **9**, 365–384 (1999).
2. G. Buzsáki, E. I. Moser, *Nat. Neurosci.* **16**, 130–138 (2013).
3. J. O'Keefe, L. Nadel, *The Hippocampus as a Cognitive Map* (Oxford Univ. Press, 1978).
4. O. Jensen, J. E. Lisman, *J. Neurophysiol.* **83**, 2602–2609 (2000).
5. C. Kentros *et al.*, *Science* **280**, 2121–2126 (1998).
6. T. J. McHugh, K. I. Blum, J. Z. Tsien, S. Tonegawa, M. A. Wilson, *Cell* **87**, 1339–1349 (1996).
7. T. J. Teyler, P. DiScenna, *Behav. Neurosci.* **100**, 147–154 (1986).
8. T. J. Teyler, J. W. Rudy, *Hippocampus* **17**, 1158–1169 (2007).
9. R. M. Grieves, K. J. Jeffery, *Behav. Processes* **135**, 113–131 (2017).
10. J. J. Kim, M. S. Fanselow, *Science* **256**, 675–677 (1992).
11. J. W. Rudy, R. C. O'Reilly, *Cogn. Affect. Behav. Neurosci.* **1**, 66–82 (2001).
12. J. F. Guzowski, B. L. McNaughton, C. A. Barnes, P. F. Worley, *Nat. Neurosci.* **2**, 1120–1124 (1999).
13. M. VanElzakker, R. D. Fevurly, T. Breindel, R. L. Spencer, *Learn. Mem.* **15**, 899–908 (2008).
14. L. G. Reijmers, B. L. Perkins, N. Matsuo, M. Mayford, *Science* **317**, 1230–1233 (2007).
15. S. Tonegawa, X. Liu, S. Ramirez, R. Redondo, *Neuron* **87**, 918–931 (2015).
16. S. A. Josselyn, S. Köhler, P. W. Frankland, *Nat. Rev. Neurosci.* **16**, 521–534 (2015).
17. K. K. Tayler, K. Z. Tanaka, L. G. Reijmers, B. J. Wiltgen, *Curr. Biol.* **23**, 99–106 (2013).
18. Local field potential and single-unit spiking were recorded during every session, as well as during pre- and postexposure rest to ensure recording stability (fig. S4).
19. L. L. Colgin *et al.*, *Nature* **462**, 353–357 (2009).
20. E. Edelmann *et al.*, *Neuron* **86**, 1041–1054 (2015).
21. B. Kuzniewska *et al.*, *Mol. Cell. Biol.* **33**, 2149–2162 (2013).
22. E. Amin, J. M. Pearce, M. W. Brown, J. P. Aggleton, *Eur. J. Neurosci.* **24**, 2611–2621 (2006).
23. T. Otto, H. Eichenbaum, S. I. Wiener, C. G. Wible, *Hippocampus* **1**, 181–192 (1991).
24. T. J. Ryan, D. S. Roy, M. Pignatelli, A. Arons, S. Tonegawa, *Science* **348**, 1007–1013 (2015).
25. K. Z. Tanaka *et al.*, *Neuron* **84**, 347–354 (2014).

ACKNOWLEDGMENTS

We thank J. P. Johansen (RIKEN CBS) and B. J. Wiltgen (UC Davis) for helpful comments on the manuscript. We thank R. Boehringer for technical support on tetrode recording, D. Polygalov for sharing scripts, M. Fujisawa and T. Tokiwa for daily assistance, the RIKEN Advanced Manufacturing Team for their assistance in microdrive production, and all the members of the Lab for Circuit and Behavioral Physiology (McHugh Lab) for advice. **Funding:** This work was supported by JSPS (Japan Society for the Promotion of Science) Grant-in-Aid for Young Scientists (B) (17K13272) (K.Z.T.), Brain Science Foundation Research Grant (K.Z.T.), the RIKEN Special Postdoctoral Researchers Program (K.Z.T.), the Uehara Memorial Foundation Research Grant (K.Z.T.), Takeda Science Foundation Visionary Research Grant (K.Z.T.), Grant-in-Aid for Scientific Research on Innovative Areas from MEXT (the Ministry of Education, Culture, Sports, Science and Technology of Japan) (17H05591, 17H05986) (T.J.M.), and RIKEN BSI and CBS (T.J.M.). **Author contributions:** K.Z.T. conceived the study and mainly conducted experiments and collected data under guidance and supervision of T.J.M. K.Z.T., H.H., and T.J.M. analyzed data. A.T. and K.N. contributed to data collection. A.J.Y.H. produced all AAV vectors. K.Z.T. and T.J.M. wrote the paper. All authors discussed and commented on the manuscript. **Competing interests:** No competing interests declared. **Data and materials availability:** All data needed to evaluate the conclusions in the paper are present in the paper or the supplementary materials. Data are archived on the servers of the Laboratory for Circuit and Behavioral Physiology at the RIKEN Center for Brain Science and are accessible at http://cbp.brain.riken.jp/tanaka_et_al.

SUPPLEMENTARY MATERIALS

www.sciencemag.org/content/361/6400/392/suppl/DC1
Materials and Methods
Figs. S1 to S8
References (*26*–*33*)

9 March 2018; accepted 20 June 2018
10.1126/science.aat5397

Science

The hippocampal engram maps experience but not place

Kazumasa Z. Tanaka, Hongshen He, Anupratap Tomar, Kazue Niisato, Arthur J. Y. Huang and Thomas J. McHugh

Science **361** (6400), 392-397.
DOI: 10.1126/science.aat5397

Support for the memory index theory

The link between contextual memory representations and locations or routes represented by hippocampal place cells during exploration remains unknown. Tanaka *et al.* examined spatial firing properties of neurons in hippocampal area CA1 on the basis of whether they had recently expressed the immediate-early activity-induced gene *c-Fos* in response to a novel context. The c-Fos–positive neurons displayed a more on-off firing pattern than the c-Fos–negative cells during context discrimination. In a contextual recognition paradigm, these results support the index theory of hippocampal function over a cognitive mapping theory.

Science, this issue p. 392